J Neuropathol Exp Neurol
Vol. 77, No. 3, March 2018, pp. 216–228
doi: 10.1093/jnen/nly010

ORIGINAL ARTICLE

Detection of Alzheimer Disease (AD)-Specific Tau Pathology in AD and NonAD Tauopathies by Immunohistochemistry With Novel Conformation-Selective Tau Antibodies

Garrett S. Gibbons, PhD, Rachel A. Banks, BA, Bumjin Kim, Lakshmi Changolkar, MS, Dawn M. Riddle, BS, Susan N. Leight, BA, David J. Irwin, MD, John Q. Trojanowski, MD, PhD, and Virginia M.Y. Lee, MBA, PhD

Abstract

Aggregation of tau into fibrillar structures within the CNS is a pathological hallmark of a clinically heterogeneous set of neurodegenerative diseases termed tauopathies. Unique misfolded conformations of tau, referred to as strains, are hypothesized to underlie the distinct neuroanatomical and cellular distribution of pathological tau aggregates. Here, we report the identification of novel tau monoclonal antibodies (mAbs) that selectively bind to an Alzheimer disease (AD)-specific conformation of pathological tau. Immunohistochemical analysis of tissue from various AD and nonAD tauopathies demonstrate selective binding of mAbs GT-7 and GT-38 to AD tau pathologies and absence of immunoreactivity for tau aggregates that are diagnostic of corticobasal degenerations (CBD), progressive supranuclear palsy (PSP), and Pick's disease (PiD). In cases with co-occurring AD tauopathy, GT-7 and GT-38 distinguish comorbid AD tau from pathological tau in frontotemporal lobar degeneration characterized by tau inclusions (FTLD-Tau), as confirmed by the presence of both 3 versus 4 microtubule-binding repeat isoforms (3R and 4R tau isoforms, respectively), in AD neurofibrillary tangles but not in the tau aggregates of CBD, PSP, or PiD. These findings support the concept of an AD-specific tau strain. The mAbs described here enable the selective detection of AD tau pathology in nonAD tauopathies.

Key Words: Alzheimer disease, Antibodies, Frontotemporal lobar degeneration, Neurodegeneration, Tauopathy.

INTRODUCTION

Tau is a microtubule binding protein expressed in the CNS where it plays an important role in the maintenance of cellular architecture and proper axonal transport (1). Six isoforms are expressed in the human brain as the result of alternative mRNA splicing that yields tau proteins containing 0–2 acidic N-terminal inserts (0 N, 1 N, or 2 N) and 3 or 4 microtubule binding repeat (MTBR) regions (2, 3). Although normally soluble and unstructured, the MTBR regions can adopt a cross-beta sheet structure forming pathological aggregates believed to cause neuronal death from toxic gain-of-function properties of oligomers/aggregates and/or loss-of-function through sequestration of tau that prevents its normal function (1, 4–6). Plausible mechanisms of tau mediated neurodegeneration due to loss of function include the disruption of axonal transport and synaptic dysfunction resulting from disturbance of tau's role in cytoskeletal regulation (1, 2, 4, 5). Development of tau aggregates may also present a physical barrier to axonal transport, while oxidative stress, induction of neuroinflammation, and synaptic dysfunction have also been suggested as mechanisms of toxic gain of function resulting from tau aggregates or oligomers (7). Nevertheless, tau dysfunction alone can result in neurodegeneration based on insights from studies of familial frontotemporal dementia (FTD) with Parkinsonism linked to chromosome 17 (FTDP-17) due to causal mutations in the tau (*MAPT*) gene (8).

The formation of insoluble tau aggregates is a pathological hallmark of Alzheimer disease (AD) and frontotemporal lobar degeneration characterized by tau inclusions (FTLD-Tau), a class of clinically and pathologically heterogeneous neurodegenerative diseases including corticobasal degenerations (CBD), progressive supranuclear palsy (PSP), and Pick's disease (PiD) (1, 9, 10). Clinically, AD and PiD manifest primarily as dementia while PSP and CBD can present with both cognitive and/or motor dysfunction. Neuropathologically, tau inclusions are present in distinct cell populations, with abundant inclusions in glial cells as well as neurons in PiD, PSP, and CBD, but tau forms almost exclusively neurofibrillary tangles (NFTs), dystrophic neurites, and neuropil threads in AD (1, 11, 12). Tau isoforms are differentially incorporated into insoluble aggregates in distinct tauopathies wherein all 6 isoforms, including both 3R and 4R are incorporated into neuronal inclusions in AD, yet PSP and CBD inclusions consist primarily of 4R tau and PiD Pick bodies consist of 3R tau

From the Department of Pathology and Laboratory Medicine, Institute on Aging and Center for Neurodegenerative Disease Research, University of Pennsylvania School of Medicine, Philadelphia, Pennsylvania (GSG, RAB, BK, LC, DMR, SNL, DJI, JQT, VMYL).
Send correspondence to: Virginia M.Y. Lee, MBA, PhD, 3600 Spruce St. 3rd Floor Maloney, Philadelphia, PA 19104; E-mail: vmylee@upenn.edu
This work was supported by NIH grants AG053036 (GSG), AG10124 (JQT), AG17586 (VMYL), and the Wyncote Foundation.
The authors have no duality or conflicts of interest to declare.
Supplementary Data can be found at http://www.jnen.oxfordjournals.org.

(13). Ultrastructural analysis reveals characteristic sizes, morphologies, and arrangements of tau filaments or tubular structures in individual tauopathies. Neuronal tau inclusions observed in AD consist of tubulofilamentous structures forming hyperphosphorylated straight (SFs) and paired helical filaments (PHFs), whereas SFs and twisted filaments are observed in CBD, PSP, and PiD (1, 14–16). The basis for how and why different tau isoforms are recruited to form the fibrillary tau inclusions in diverse tauopathies is unknown, but insights into these questions will contribute to our understanding of the generation of unique tau strains which appear to undergo differential cell-to-cell spread (17–23). Indeed, if the recent cryo-electron microscopy observations of AD SFs and PHFs can be extended to the tau inclusions of PiD, PSP, CBD, and other tauopathies, these studies may disclose the structural basis for different strains of tau pathology (24).

Tau inclusions observed in the absence of additional pathological features such as deposits of amyloid-beta (Aβ) peptides have been suggested to deserve a distinct pathological classification termed primary age-related tauopathy or PART (25), and they contain both 3R and 4R tau isoforms that are comprised of typical AD-like PHFs (26, 27). Clinically, PART cases range from normal to mild cognitive impairment with rare cases of severe impairment (25). However, the common occurrence of comorbid neurodegenerative diseases in the aged population confounds systemic characterization of the clinicopathological spectrum in these individuals. It has also been posited that there is insufficient evidence at this time to classify PART as a distinct pathological entity and it is debated whether or not PART represents an early stage of AD with low levels of Aβ pathology or a stage before Aβ pathology is apparent (28). Therefore, it is unknown whether PART represents a benign or protective mechanism of normal aging or whether it is "on pathway" to a tauopathy, and may later develop into AD (25, 28).

Mounting evidence suggests that unique tau strains may be responsible for the distinguishing features of different tauopathies (17–22). Intracerebral injection of human brain-derived pathological tau extracts into the brains of mice led to the templated spread or propagation of morphologically distinct tau pathologies that phenocopy the corresponding tauopathies (i.e. AD, CBD, PSP, PiD) in transgenic (Tg) mice (17, 18). Injection of NFT enriched AD brain-lysate into nonTg mice resulted in tau aggregates that spread to neuroanatomically connected brain regions, whereas brain injections of synthetic tau preformed fibrils (PFFs) did not seed endogenous mouse tau aggregates supporting the notion for the existence of AD and nonAD specific tau conformation(s) or strain(s) (29). Importantly, human brain-derived tau extracts from AD, CBD, and PSP induce cell-type specific tau pathology upon intracerebral injection into nonTg mice (23). Together, these findings support the presence of AD, CBD, and PSP specific strains of pathological tau that can be stably extracted and transmitted in vivo.

Numerous antibodies have been produced that recognize linear tau amino acid sequences, as well as tau epitopes that are phosphorylation or acetylation dependent, while other epitopes reflect oligomeric tau species and/or distinct conformations of pathological tau. For example, MC1 and ALZ50 are monoclonal antibodies (mAbs) that recognize conformation-dependent epitopes in tau consisting of amino acid residues 7–9 and 312–341 (30, 31). Tau-66 recognizes discontinuous epitopes comprised of residues 155–244 and 305–314 of the tau molecule that are not specific to pathological conformations and are recognized in native recombinant tau protein, likely representing transient secondary structures (32). TG3 recognizes a local peptide conformational change around phosphorylated Thr231 of tau that is present in AD tissue yet is also generated by in vitro phosphorylation of recombinant tau protein by the kinase p34cdc2 (33, 34). Commercially available 3R and 4R tau isoform-specific antibodies have been previously utilized to investigate tau isoform composition in tauopathies and support the findings that PiD primarily consists of 3R tau while CBD and PSP tau inclusions consist of 4R tau; however, some heterogeneity in these studies may reflect nonspecific background or tissue fixation and antigen retrieval conditions (35). Furthermore, the antibody 12E8, which detects phospho-Ser262/Ser356 tau, was initially employed to discern between PiD and CBD and the epitope was thought to be present in CBD tau aggregates but absent in PiD (36). However, 12E8 turns out to be fixation-dependent and detected both 3R and 4R tau aggregates (37, 38). Despite the abundance of conformation selective, isoform specific, and phospho-specific tau antibodies, to our knowledge, none of these antibodies or other molecular tools differentiate disease-specific strains of tau.

Thus, the aim of our study was to develop novel mAbs against human brain-derived AD PHFs and seeded recombinant tau PFFs that can distinguish conformationally distinct strains of pathological tau. Here, we show that novel conformation-selective tau mAbs recognize AD-specific tau pathology but not the tau inclusions found in PiD, PSP, and CBD in postmortem human brain tissues by immunohistochemistry (IHC). Conformation-dependent binding to AD brain extracted pathological tau further supports the specificity of novel tau strain-specific mAbs. These mAbs represent unique reagents to distinguish AD tau pathology from tau inclusions in PiD, PSP, and CBD.

MATERIALS AND METHODS

Tau PHF Extraction From AD Brain

Tau PHFs were extracted from AD human brain tissue from the Center for Neurodegenerative Disease Research brain bank, as described (29, 39, 40). Briefly, cortical gray matter was homogenized in 10 mM Tris pH 7.4, 0.8 M NaCl, 1 mM EDTA, 2 mM DTT, with protease inhibitors, phosphatase inhibitors, and 1 mM PMSF, 0.1% sarkosyl, and 10% sucrose. Following a low speed centrifugation at 10 000 *g* for 10 minutes at 4°C, the supernatant sarkosyl concentration was increased to 1% and centrifuged at 300 000 *g* for 1 hour at 4°C. The pellet containing pathological tau was washed with PBS, briefly sonicated and centrifuged for 100 000 *g* for 30 minutes at 4°C. The resultant pellet was resuspended in PBS, sonicated and subjected to low-speed spin of 10 000 *g* for 30 minutes at 4°C providing supernatant containing enriched AD tau PHFs. Soluble tau analyzed by dot blot was derived from supernatant

of homogenized brain containing 0.1% sarkosyl dialyzed into 10 mM Tris pH 7.4, 0.8 M NaCl, 1 mM EDTA, 2 mM DTT and centrifuged 100 000*g* for 30 minutes at 4°C. Tau levels in brain derived extracts were calculated using the Tau5 sandwich ELISA assay with serial dilutions of recombinant T40 tau protein to generate a standard curve, as previously described (41).

In Vitro Seeded Fibrillization of Recombinant Tau

Full-length human T40 (2N4R) tau was expressed in BL21 (DE3) RIL cells and purified by cation exchange chromatography as described (42). AD-seeded recombinant tau PFFs were prepared as described (29) with 4 μM of AD tau PHFs (estimated from average molecular weight of 6 tau isoforms), and 36 μM recombinant T40 tau in dPBS and 2 mM DTT. Fibrillization mixtures were shaken at 1000 RPM at 37°C for 3 days. Fibrillization was confirmed by sedimentation assay; an aliquot of the fibrillization mixture was centrifuged 100 000 *g* for 30 minutes at 4°C, the supernatant and pellet were individually collected and analyzed by SDS-PAGE followed by Coomassie Blue staining.

Antibody Production

Tau PHFs from AD brain and AD-seeded recombinant PFFs were used separately as immunogens for subcutaneous injections emulsified with complete Freund's adjuvant (25 μg tau/mouse) followed by 2 subsequent boosts of 25 μg tau emulsified with incomplete Freund's adjuvant 3 and 6 weeks following the initial injections, as previously described (43). Nine weeks after initial antigen injection, mouse spleens were dissociated into single cell suspensions and fused with SP2 cells by 1-minute treatment with polyethylene glycol. Hybridoma cells were cultured in Kennett's HY (90% DMEM, 10% NCTC135, glucose, glutamine, pH 7.4 $NaHCO_3$), 20% fetal bovine serum (FBS), 1% L-glutamine, 1% Pen/strep, OPI (oxoloacetate, pyruvate, insulin) 4 μg/mL, azaserine hypoxanthine, 10% fresh filtered SP2 conditioned media, 10% thymus supernatant. Monoclonal populations were isolated by limiting dilution to 0.3 cells/well in 96-well plates. Antibody producing clones were screened and verified by tau direct ELISA and IHC conducted in human AD tissue. After 2 rounds of subcloning, 2 mAbs designated as GT-7 and GT-38 were purified from cell culture supernatants with Magne Protein A/G beads (Promega, Sunnyvale, CA). All procedures were approved by the University of Pennsylvania Institutional Animal Care and Use Committee (IACUC) and performed according to the *NIH Guide for the Care and Use of Experimental Animals*.

IHC

All human brain tissue samples used in this study were obtained at autopsy, ethanol-fixed, paraffin-embedded, and cut into 6 μm thick sections and characterized, as described (44, 45). For IHC staining, sections were deparaffinized in xylene and rehydrated in ethanol (100%–70%) as reported previously (38, 46, 47). Tau antibodies PHF-1 (gift of Peter Davies) 1:5000, without antigen retrieval while GT-7 and GT-38 at 0.4 μg/mL diluted in 2% FBS in 50 mM Tris pH 7.2, RD3 specific for 3R tau (Millipore 05-803, Millipore, Billerica, MA) 1:5000, and RD4 specific for 4R tau (Millipore 05-804) 1:5000 immunostaining was carried out following antigen retrieval by citric acid unmasking solution (Vector H-3300, Vector Laboratories, Burlingame, CA) heated at 95°C for 15 minutes. Antibody binding was detected by Super Sensitive Polymer-HRP (QD420-YIK, BioGenex, San Ramon, CA) followed by DAB peroxidase substrate (Vector SK4105).

Sandwich ELISA

Tau5, GT-7, and GT-38 were each coated onto MaxiSorp 96-well plates (Thermo Fisher 12565347, Thermo Fisher, Waltham, MA) at 75 ng/well in 0.1 M $NaHCO_3$ pH 9.6 buffer for 18 hours at 4°C, washed with PBS containing 0.1% Tween-20, blocked with Block Ace solution (AbD Serotec, Hercules, CA) for more than 24 hours at 4°C and exposed to tauopathy brain derived extracts in 0.2% BSA in PBS. Tau binding was detected with the biotin-conjugated antitau antibodies BT2 (Thermo Scientific MN1010B) and HT7 (Thermo Scientific MN1000B) used in combination followed by detection with streptavidin conjugated HRP (Thermo Scientific 21130) and colorimetric development with TMB peroxidase substrate (KPL 50-76-03) quenched with 10% phosphoric acid, and absorbance measurements at 450 nm as previously described (41).

Dot Blot

Total homogenates containing pathological tau extracted from AD midfrontal cortex were denatured in 0.2 M guanidine HCl 2 hours at room temperature and were diluted in Tris-buffered saline (TBS) for sample application. Alternatively, insoluble and soluble tau derived from brain extracts of various tauopathies were prepared as described above. Samples were immobilized on 0.2 μm nitrocellulose membrane by vacuum. The membrane was stained with Ponceau S (P3504, Sigma, St. Louis, MO), washed with water, and scanned, then blocked with 5% nonfat milk in TBS containing 0.1% Tween-20 (TBST). Dot blot was performed with tau antibodies K9JA 1:5000 (A0024, Dako, Carpinteria, CA), MC1 (gift of Peter Davies) GT-7 or GT-38 4 μg/mL respectively diluted in 5% nonfat milk in TBST followed by secondary detection with goat antirabbit (Li-Cor 926-68071) or goat antimouse (Li-Cor 926-32210) infrared dye conjugated antibodies imaged on Odyssey Imaging System.

Dephosphorylation of AD Tissue

Ethanol-fixed, paraffin-embedded AD tissue was sectioned and rehydrated followed by citric acid antigen retrieval as described above. Tissue was enzymatically dephosphorylated by calf intestinal phosphatase (CIP) (M0290S, New England BioLabs, Ipswich, MA) diluted to 33 U/mL in 50 mM Tris pH 7.6, 100 mM NaCl, 10 mM $MgCl_2$, 1 mM DTT and incubated for 2 hours at 37°C. Tissue was rinsed in 50 mM Tris pH 7.2 and sequentially dephosphorylated with λ-phosphatase (New England BioLabs P0753S) at 650 U/mL in PMP buffer (New England BioLabs B0761S) with 1 mM $MnCl_2$.

RESULTS

Novel Antibodies Selectively Recognize Pathological AD Tau

To neuropathologically distinguish an AD-specific tau strain, we generated novel tau mAbs that detect AD tau pathology by IHC but not the tau inclusions in the other tauopathies studied. Mice were immunized with brain-derived AD tau PHFs, extracted from frontal cortex gray matter of an AD case selected based on high pathological tau burden and absence of α-synuclein or TDP-43 inclusions, or recombinant tau PFFs seeded by AD-brain extract (AD-PFFs), as described (29). To identify mAbs specific for pathological AD tau, hybridoma supernatants were screened by IHC staining of slides containing regions of high pathological tau burden from cases of AD, CBD, PSP, and PiD combined into a single paraffin block. Utilizing this approach, we identified 2 hybridoma clones, GT-7 and GT-38, that selectively recognized tau pathology in AD but not CBD, PSP, or PiD. Interestingly, the GT-7 clone was isolated from a mouse immunized with AD-seeded recombinant tau PFFs and the GT-38 clone was isolated from a mouse immunized with tau PHFs from AD brain. Hybridomas expressing selective antibodies were cloned twice to monoclonal populations and we assessed the stability and reproducibility of GT-7 and GT-38 clones. Frozen cells stocks, once thawed, recovered and maintained mAb expression. We verified that purified GT-7 and GT-38 IgG_1 mAbs selectively recognized tau pathology in AD but not CBD, PSP, or PiD by staining angular gyrus from each tauopathy brain containing a high pathological tau burden (Fig. 1). As observed with other antibodies, tissue fixation conditions influenced sensitivity and background revealing that GT-7 and GT-38 preferentially detect tau in ethanol-fixed tissue with lower background than in formalin-fixed tissue, therefore all tauopathies and brain regions tested by IHC were ethanol-fixed (38). In contrast to GT-7 and GT-38 mAbs, the conformation-selective tau mAb MC1, in addition to the phosphorylation-dependent PHF1 mAb, robustly detected tau aggregates in all tested tauopathies (Supplementary Data Fig. S1). The selectivity of GT-7 and GT-38 were further verified by IHC staining of additional cases of AD (n = 14), CBD (n = 10), PSP (n = 11), and PiD (n = 8) (Table; Supplementary Data Table S1).

In AD tissue, GT-7 and GT-38 predominantly bound NFTs but also detected neuritic tau pathology surrounding Aβ plaques and thick neuropil threads (Supplementary Data Fig. S2). To rule out the possibility that AD selectivity resulted from epitope shielding, we assessed the binding of GT-7 and GT-38 in multiple tauopathies following formic acid and citric acid/microwave antigen retrieval techniques, which have been shown to "unmask" tau epitopes (47). These additional treatments had no effect on the detection of tau pathology for either mAb in CBD, PSP, or PiD but improved the signal for GT-38 in AD (Supplementary Data Fig. S3). To assess the selectivity of GT-7 and GT-38 in other brain regions with tau pathology further, dentate gyrus from PiD and substantia nigra from PSP were IHC stained (Supplementary Data Fig. S4). GT-7 and GT-38 were both negative for staining of dense Pick bodies observed in PiD. In the substantia nigra of PSP cases, pigmented cells were observed and 4R tau containing inclusions were observed but GT-7 was completely negative and GT-38 stained an occasional rare neuropil thread.

To verify the selective recognition of tau strains biochemically, GT-7 and GT-38 were used as capture antibodies in a sandwich ELISA format to immunocapture tau derived from insoluble pathological tau extracted from AD, CBD, and PSP brains. Consistent with IHC, GT-7, and GT-38 selectively immunocaptured tau from AD brain compared with CBD or PSP brain-derived extracts (Fig. 2A, B). GT-7 showed slightly greater selectivity and GT-38 showed partial binding to CBD and PSP brain-derived tau. The pan-tau antibody Tau5, which recognizes the linear peptide sequence of tau between amino acids 210–230, was used as a loading control to demonstrate that equivalent levels of tau were present in tauopathy extracts and that the detection antibody combination comprised of BT2/HT7 detects tau from each of the tauopathy extracts, demonstrating that selectivity results from the capture antibodies GT-7 and GT-38 (Fig. 2C). To verify the selectivity of GT-7 and GT-38 further, soluble and insoluble fractions of tau derived from AD, CBD, and PSP brains were immobilized onto nitrocellulose membrane and immunoblotted with the respective mAbs (Fig. 2D). Loading of brain-derived tau extracts was normalized based on pan-tau, K9JA, signal and MC1 was used as a conformation-selective control to indicate pathological tau. GT-7 and GT-38 barely detected AD tau in the soluble extract but the majority of immunoreactivity was observed in the insoluble tau fractions, consistent with MC1. Importantly, both mAbs GT-7 and GT-38 selectively recognized pathological insoluble tau from AD brains compared with CBD and PSP brain-derived tau by dot blot, in agreement with the sandwich ELISA and IHC results. Together, these results support the binding of GT-7 and GT-38 to conformations of tau found predominantly in AD compared with CBD and PSP.

GT-7 and GT-38 Recognize Preclinical AD Tau Aggregates in Cognitively Normal and PART Brain Tissue

On the basis of the intriguing possibility that novel tau mAbs GT-7 and GT-38 recognize a distinct strain of tau found in AD, we investigated whether the mAbs detected tau aggregates in cognitively normal controls and PART cases. Because aged individuals with no cognitive impairment can exhibit tau pathology, we assessed the entorhinal cortex of cognitively normal controls and PART subjects. Interestingly, GT-7 and GT-38 detected tau pathology in the entorhinal cortex of individuals with no cognitive impairment and PART (Fig. 3). To assess the similarity of the tangles observed in normal and PART cases to AD, (which contain both 3R and 4R tau), tissue sections were stained with 3R tau- and 4R tau-specific antibodies, as described (38). We observed that GT-7 and GT-38 detected NFTs that are also recognized by mAbs specific to 3R and 4R tau, respectively. These findings support the notion that NFTs present in cognitively normal and PART cases may represent preclinical AD pathology, containing both 3R and 4R tau isoforms and adopting an AD tau pathology-specific conformation recognized by GT-7 and GT-38.

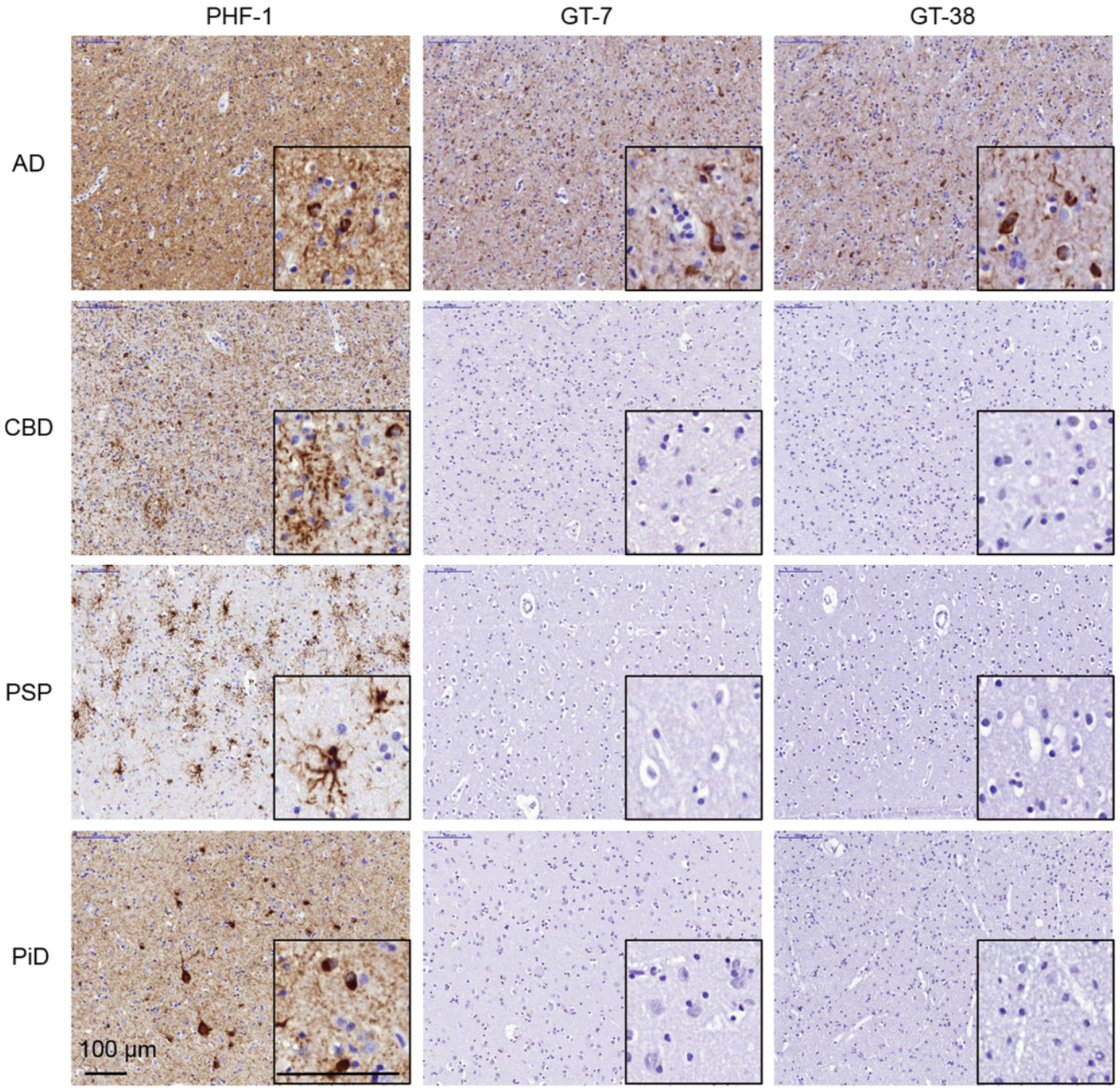

FIGURE 1. Novel tau mAbs selectively detect AD tau pathology but are not immunoreactive with tau aggregates that are diagnostic of nonAD tauopathies by IHC. Fixed, paraffin-embedded tissue from AD, CBD, PSP, and PiD angular gyrus were stained by IHC with antipSer396/pSer404 tau PHF1or novel AD-specific tau mAbs GT-7 and GT-38.

Differentiation of Comorbid AD in the Presence of Various Tauopathies

Because the entorhinal cortex of normal controls contained tau pathology, we investigated whether AD, CBD, PSP, and PiD entorhinal cortex and hippocampus also contained tau pathology immunoreactive with GT-7 and GT-38. Interestingly, we detected GT-7 and GT-38 immunoreactivity in the entorhinal cortex and hippocampus CA1 of a subset of CBD and PSP cases (Fig. 4). To assess whether GT-7 and GT-38 staining in the hippocampus of patients with a primary diagnosis of CBD or PSP was due to comorbid AD pathology, we examined the isoform composition of tangles present in the hippocampus. We found that in cases of pure 4R tauopathy, GT-7 and GT-38 were completely negative, whereas both antibodies detected tangles that contained 3R and 4R tau isoforms in the entorhinal cortex and hippocampus CA1. To test whether GT-7 and GT-38 are 3R tau-specific, we stained pure 3R tau PiD cases and found that IHC staining of both GT-7 and GT-38 was absent and therefore they did not detect Pick bodies (Fig. 4). To verify whether GT-7 and GT-38

TABLE. Summary of Cases for Characterization of GT-7 and GT-38

Case ID	Neuropathological Diagnosis	Clinical Diagnosis	Sex	Age at Death (Years)	Duration of Symptoms (Years)	MMSE/Clinical Dementia Rating Score (0–30/0–3)	Braak Stage (0–3)	CERAD Score (0–3)
110100	AD	AD Probable	F	68	8	14/3	3	3
115892	AD	AD Possible	M	88	11	19/3	2	3
106239	AD	AD Probable	M	84	7	24/2	3	3
107536	AD	FTLD-NOS	F	65	13	–/–	3	3
100666	AD	AD probable	F	76	8	–/–	3	3
107718	AD	AD probable	M	84	15	11/2	3	3
107696	AD	AD probable	F	80	12	–/–	3	3
112648	AD	AD probable	M	85	12	–/–	2	3
105398	AD	PD	M	84	19	–/–	2	2
108441	AD	PD	F	77	4	–/–	2	1
100440	AD	AD probable	M	70		1/2	3	3
112403	AD	AD probable	M	71	8	14/3	3	3
106761	AD	AD probable	F	73	9	–/–	3	3
110674	AD	AD probable	F	59	9	24/1	3	3
106229	AD	AD probable	F	87	18	–/–	3	3
111881	AD	AD probable	M	66	11	1/3	3	3
112964	CBD	DLB	F	74	7	–/–	N/A	0
105358	CBD	PPA (logopenic)	M	68	5	–/–	N/A	1
107516	CBD	bvFTD-FTLD	M	52	3	–/–	N/A	0
104281	CBD	FTD-NOS	F	59	2	15/-	N/A	0
114762	CBD	PSP	F	59	5	–/–	N/A	1
108196	CBD	Corticobasal syndrome	F	66	8	–/–	N/A	0
116508	CBD	Corticobasal syndrome	F	85	9	–/–	N/A	1
102149	CBD	PPA (PNFA)	F	56	6	–/–	N/A	0
118323	CBD	CBD	F	80	4	–/0.5	N/A	–
111005	CBD	FTLD-NOS	M	44	–	18/-	N/A	1
114348	PSP	FTD-NOS	M	84	8	17/3	N/A	3
111530	PSP	PPA (PNFA)	M	79	9	–/–	N/A	0
106959	PSP	–	F	77	–	–/–	N/A	0
112401	PSP	CBD	F	71	10	16/2	N/A	0
101483	PSP	Multiple	M	68	8	28/0.5	N/A	0
114511	PSP	PSP	M	79	9	–/–	N/A	2
103782	PSP	CBD	F	80	5	–/–	N/A	2
104282	PSP	CBD	F	65	6	–/–	N/A	2
110181	PSP	PSP	F	63	5	–/–	N/A	0
101407	PSP	CBD	F	78	3	–/–	N/A	0
107667	PiD	–	M	59	–	–/–	N/A	0
111853	PiD	bvFTD-FTLD	M	76	8	–/–	N/A	0
105564	PiD	bvFTD-FTLD	M	57	9	–/–	N/A	0
107187	PiD	FTLD-NOS	F	84	14	11/-	N/A	1
106309	PiD	bvFTD-FTLD	M	71	13	–/–	N/A	0
106814	PiD	bvFTD-FTLD	M	72	15	–/–	N/A	0
108508	PiD	PPA (semantic dementia)	M	71	17	–/–	N/A	0
115001	PiD	bvFTD-FTLD	M	58	4	–/–	N/A	4
118624	PART (possible)	Normal	M	70	–	–/–	1	0
118648	PART (definite)	Normal	M	73	–	–/–	1	0
112090	PART (definite)	Normal	F	83	–	28/0	1	0
118375	Normal	Normal	M	52	–	–/–	0	0
103053	Normal	Normal	F	83	–	–/–	–	1
106711	Normal	Normal	F	56	–	–/–	1	0
102391	Normal	Schizophrenia	M	83	–	–/–	1	0

(continued)

TABLE. Continued

Case ID	Neuropathological Diagnosis	Clinical Diagnosis	Sex	Age at Death (Years)	Duration of Symptoms (Years)	MMSE/Clinical Dementia Rating Score (0–30/0–3)	Braak Stage (0–3)	CERAD Score (0–3)
104057.01	AD (no cognitive impairment)	Normal	M	94	–	30/0	1	2
118446	AD (no cognitive impairment)	Normal	M	93	–	30/0	3	1
106960	AD (no cognitive impairment)	Normal	M	80	–	–/–	2	2

The neuropathological diagnosis, clinical diagnosis, sex, age, disease duration, MMSE score (0–30)/Clinical dementia rating score (0–3), Braak stage (0–3), and CERAD score (0–3) are shown for all tauopathy and no cognitive impairment controls used to characterize the selectivity of GT-7 and GT-38 by IHC, ELISA, and dot blot. Abbreviations: F, female; M, male; CERAD, Consortium to Establish a Registry for Alzheimer's Disease; MMSE, Mini-mental state examination; AD, Alzheimer disease; CBD, corticobasal degeneration; PSP, progressive supranuclear palsy; PiD, Pick's disease; DLB, dementia with Lewy bodies; bvFTD-FTLD, behavioral variant frontotemporal dementia with frontotemporal lobar degeneration; NOS, not otherwise specified; PART, primary age related tauopathy; PPA, primary progressive aphasia; PNFA, progressive nonfluent aphasia; N/A, not applicable. Tau extracted from case 110100 was used as the antigen for antibody development.

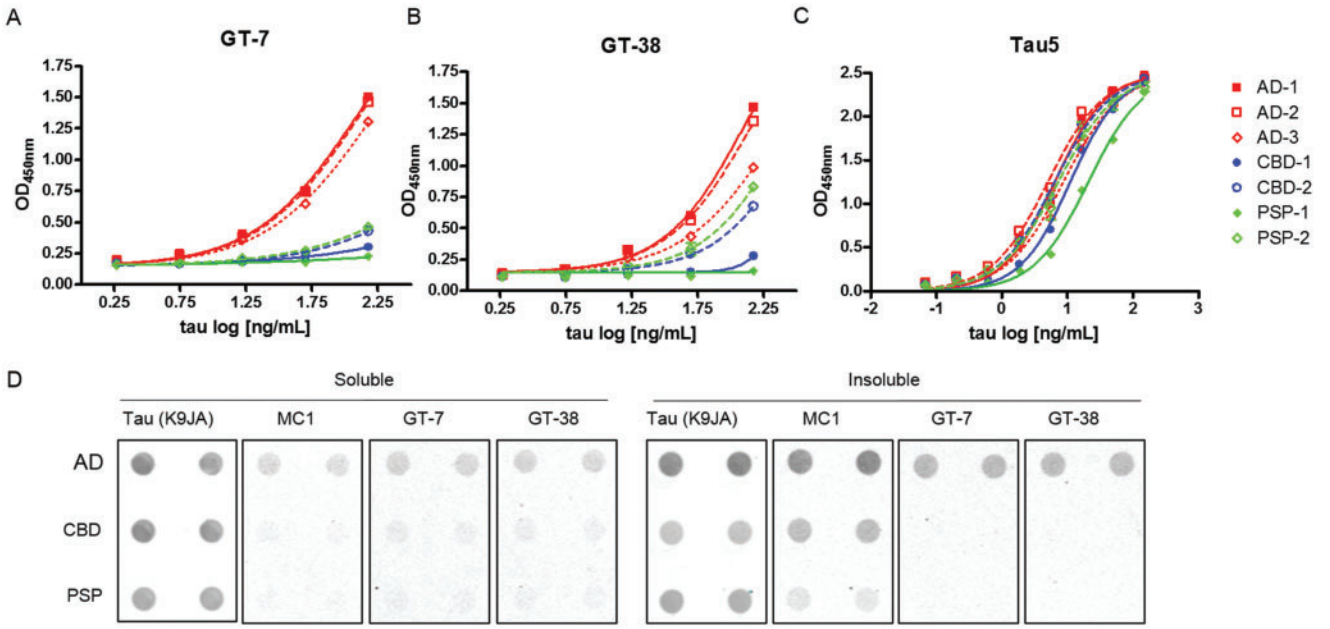

FIGURE 2. Tau mAbs selectively detect pathological tau from AD brains. **(A–C)** Sandwich ELISA assay with capture antibodies **(A)** GT-7, **(B)** GT-38, and **(C)** Tau5 capture tau from brain-derived extracts of several cases of each tauopathy, AD, CBD, and PSP. The biotinylated pan-tau BT2 and HT7 antibodies were used to detect immunocaptured tau. **(D)** Dot blot analysis of soluble and insoluble tau from brain extracts of several tauopathies probed with the pan-tau loading control antibody K9JA, conformation-selective MC1, or novel mAbs GT-7 and GT-38. The rabbit polyclonal pan-tau antibody K9JA enabled simultaneous immunoblotting with GT-7 and GT-38 using antimouse and antirabbit IR-dye conjugated secondary antibodies to ensure equivalent nitrocellulose immobilization of tau across samples. PiD brain derived extracts were not evaluated due to limiting concentrations of pathological tau present.

immunoreactivity in CBD and PSP cases can be attributed to comorbid AD, we performed co-immunofluorescence staining with Thioflavin S (ThioS). PSP and CBD tauopathy are largely nonreactive to amyloid-binding dyes such as ThioS; therefore, the inability of GT-7 and GT-38 to detect 4R tau pathology when compared with robust signal in detecting mature AD NFTs suggest these mAbs can be used to differentiate AD copathology in FTLD-Tau (48, 49). We also found that GT-7 and GT-38 staining completely colocalized with ThioS signal indicating that they bind to AD NFTs co-occurring with the primary diagnostic tau pathology of nonAD tauopathies (Fig. 5). Together, these findings demonstrate that GT-7 and GT-38 distinguish ThioS-, 3R-, and 4R-containing AD NFTs from CBD, PiD and PSP tau pathology.

Conformation-Dependent Binding to Tau

To determine the molecular features of distinct tau strains responsible for AD-selective antibody binding, we investigated whether disruption of protein conformation of AD NFTs influenced binding of GT-7 and GT-38. Tau enriched AD brain extracts were chemically denatured by guanidine hydrochloride (GuHCl) and binding of GT-7 and GT-38 was assessed by dot blot assay. Ponceau S staining and the control

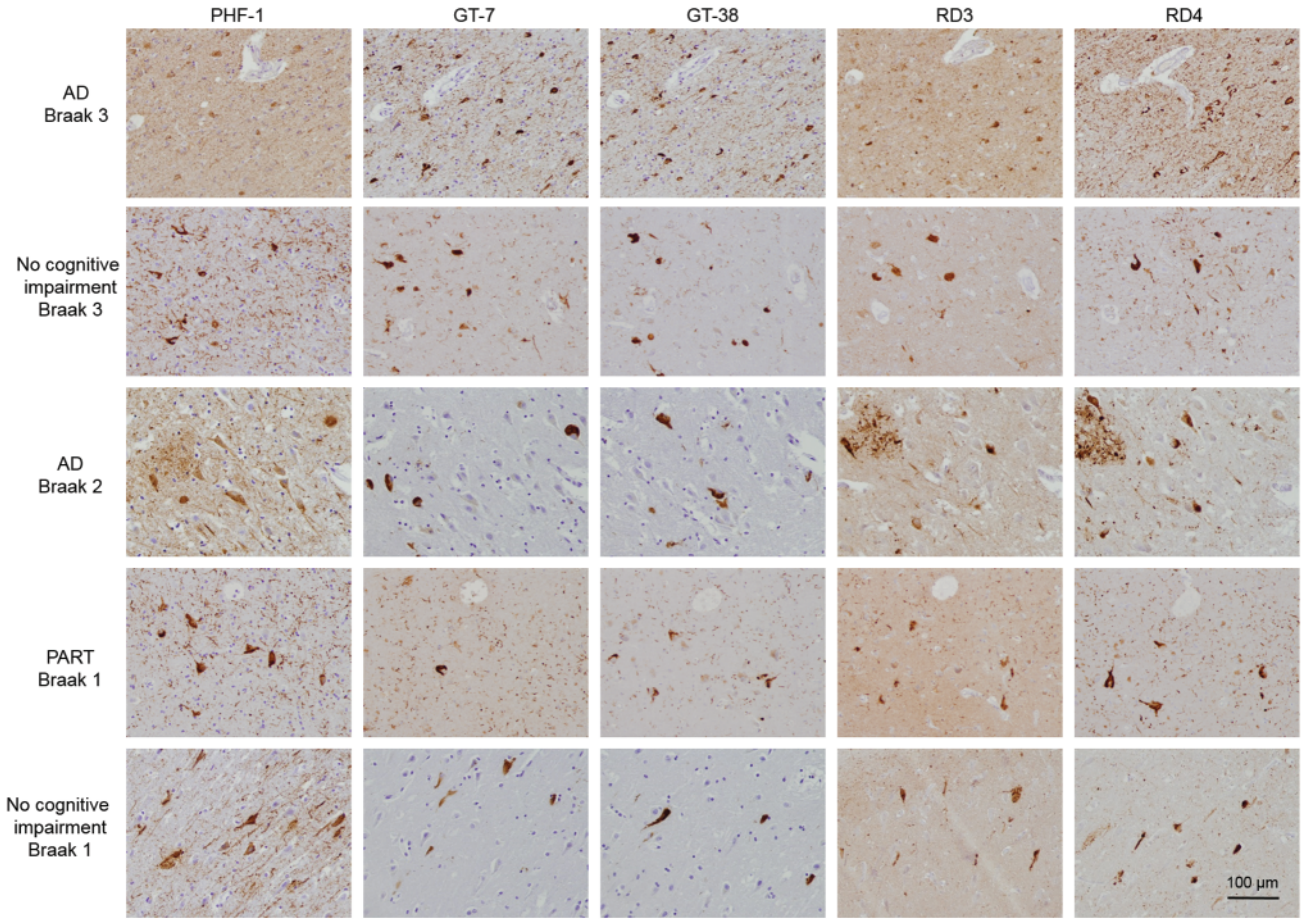

FIGURE 3. GT-7 and GT-38 immunostain 3R and 4R containing tau inclusions in cognitively normal and PART cases. Fixed, paraffin-embedded tissue from AD, PART, and no cognitive impairment control entorhinal cortex were stained by IHC with PHF1, novel tau mAbs GT-7 or GT-38, 3R tau specific RD3, or 4R tau specific RD4.

rabbit polyclonal tau antibody K9JA were used as loading controls to assess the effect of GuHCl denaturation on the immobilization of tau onto nitrocellulose membrane (Fig. 6A). Consistent with a conformation-dependent epitope, GT-7 and GT-38 binding was significantly diminished following chemical denaturation of AD tau (Fig. 6B). This finding suggests that GT-7 and GT-38 recognize an AD tau pathology strain-specific conformation of pathological tau.

To further support the conformational dependence of GT-7 and GT-38 binding to AD tau and rule out dependence on posttranslational modification such as phosphorylation, we performed IHC on AD tissue following sequential dephosphorylation. CIP and λ-phosphatase treated AD tissue resulted in loss of binding of phospho-tau specific antibodies AT8 and AT180 but did not affect the immunoreactivity of GT-7 or GT-38 (Fig. 6C). These data provide evidence that GT-7 and GT-38 binding does not depend on phosphorylation of tau in AD and supports the interpretation of conformation-dependent binding.

DISCUSSION

Here, we report the generation of 2 novel conformation-selective tau mAbs, GT-7 and GT-38, that specifically recognize AD tau pathology in human brain tissue. Tau NFTs are comprised of misfolded tau proteins including all 6 tau isoforms that undergo a maturation process executed via post-translational modification, conformation change, and cleavage events although tau PFFs can form in the absence of any post-translational modification (50, 51). Serine and threonine hyperphosphorylation occurs early in tau aggregate formation by reducing binding to microtubules thereby increasing the soluble tau concentration that precede aggregation of tau (50, 52–55). Phosphorylation of tyrosine residues can occur in tau within NFTs but they are excluded from neuropil threads and dystrophic neurites demonstrating differential phosphorylation states of tau within maturing aggregates (56). Similarly, GT-7 and GT-38 preferentially recognize NFTs compared with neuropil threads and dystrophic neurites, and therefore they are dissimilar from the staining pattern of phospho-tau antibody PHF1, which labels phosphorylated Ser396/Ser404 which are abundant in neuropil threads (57). As opposed to pathological modifications that generate novel epitopes for antibody recognition, phosphorylation can also prevent binding of antibodies such as BT2 upon phosphorylation of Ser199 and or Ser202 (58, 59). However, GT-7 and GT-38 detection of tau

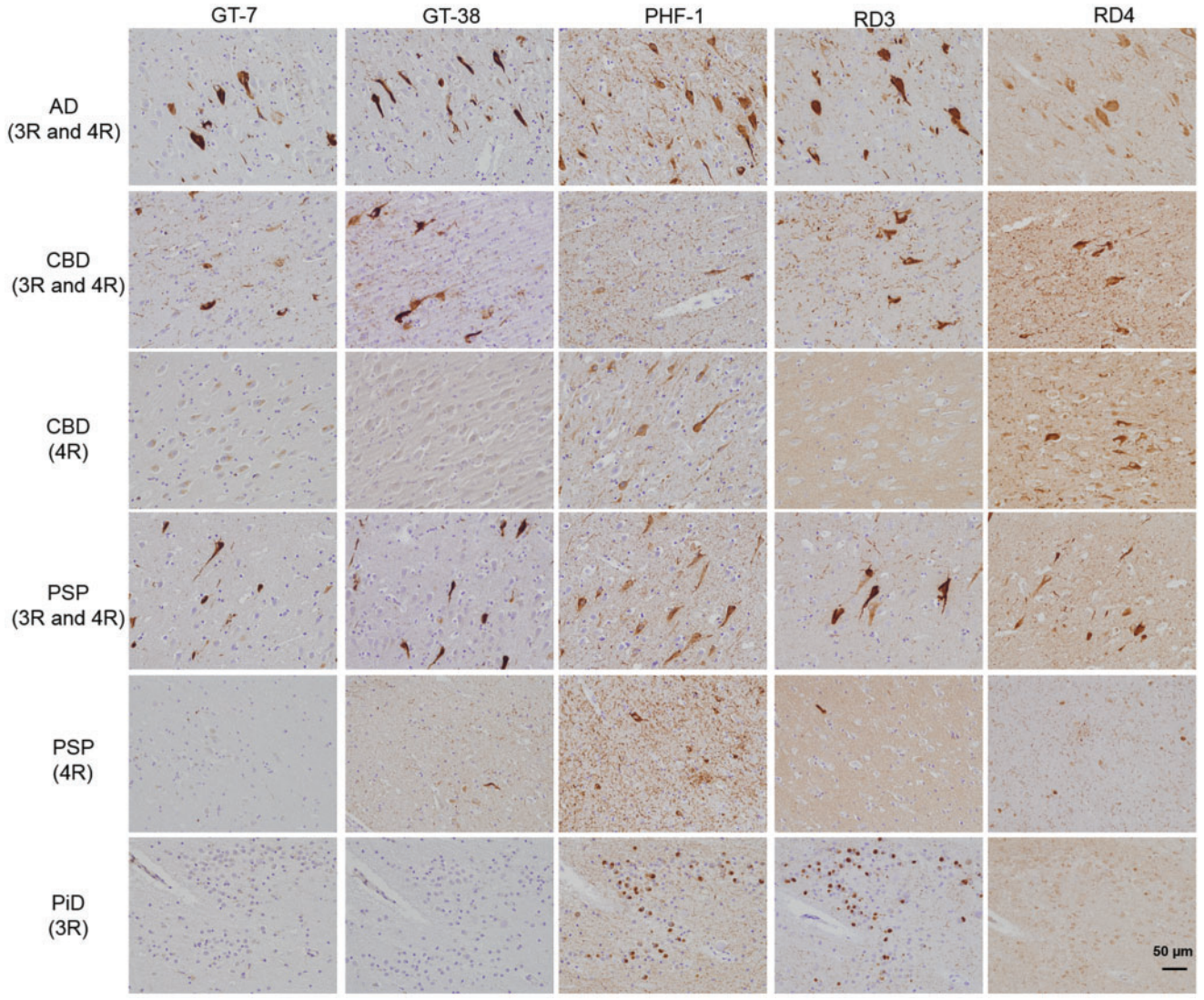

FIGURE 4. GT-7 and GT-38 differentiate comorbid AD tau pathology in the presence of nonAD tauopathies. Fixed, paraffin-embedded tissue from AD, CBD, PSP, and PiD hippocampus were immunohistochemically stained with, GT-7, GT-38, PHF1, RD3, and RD4.

pathology was not influenced by dephosphorylation of AD tau in human tissue sections, providing additional evidence that they bind to a complex conformational epitope. In the maturation of tau NFTs, distinct conformational changes result in the folding of the N-terminus to interact with the MTBR portion of tau creating the ALZ50/MC1 epitope (30, 31); this observation is supported by the recent report of the molecular-resolution structure of tau in SFs and PHFs deciphered by cryo-EM (24). Furthermore, there are ordered structural changes to tau fibrils resulting in additional pathological conformations of tau within AD NFTs demonstrated by the lack of colocalization of ALZ50 and Tau-66 measured by confocal co-immunofluorescence (60). GT-7 and GT-38 display exquisite selectivity for AD tau pathology by IHC, suggesting they recognize distinct epitopes from previously reported conformation-selective tau mAbs, ALZ50, MC1, and Tau-66, considering their respective promiscuity among tauopathies (61, 62). Lastly, mature NFTs undergo further posttranslational modification including acetylation at lysine K280 and truncation by cleavage at glutamate E391 and aspartate D421 (63–67).

Emerging evidence suggests that the heterogeneous phenotypes and cell-type distribution of tau aggregates in tauopathies are due to unique tau strains (17–22, 29). Biochemical characterization of tau derived from major human tauopathies demonstrate differential susceptibility to proteases suggesting unique conformations and isoform composition contribute to defining features of distinct strains (68). Our data are in agreement with the strain hypothesis of different pathological species of tau by demonstrating that GT-7 and GT-38 selectively immunocapture pathological tau in AD brain-derived extracts compared with CBD and PSP supporting the notion that they

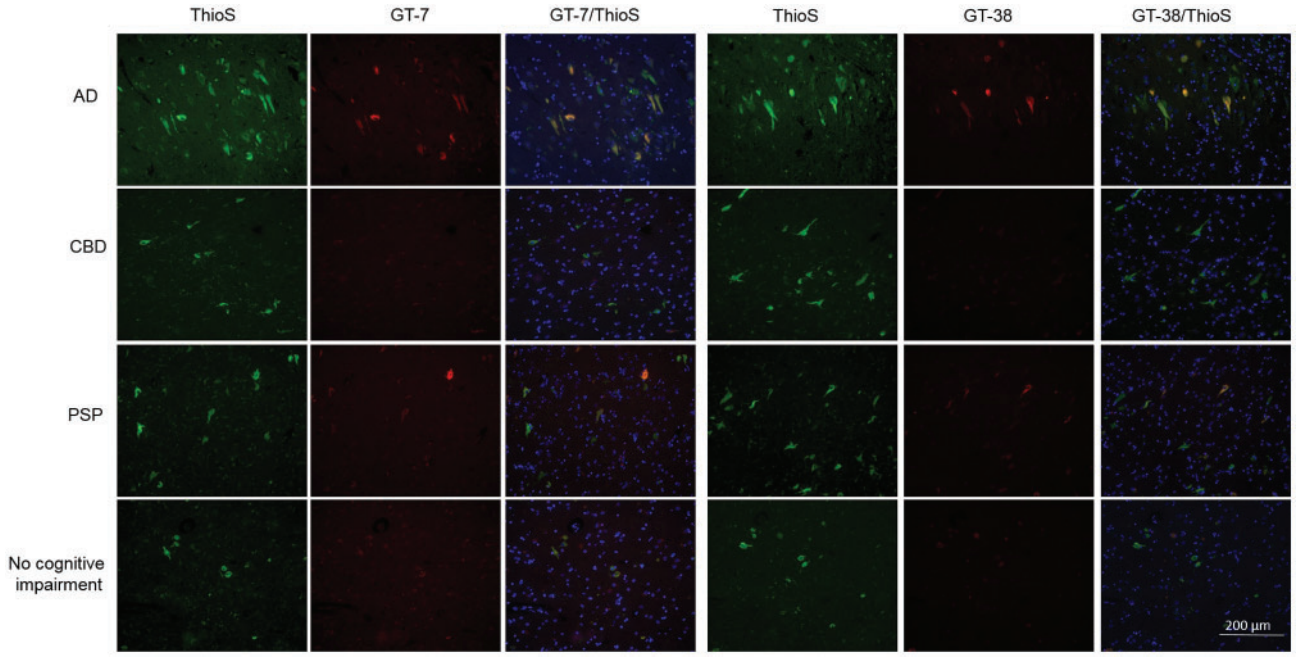

FIGURE 5. GT-7 and GT-38 detect ThioS-positive tau aggregates in tauopathies. Co-immunofluorescent staining of AD, CBD, PSP and cognitively normal patient hippocampal tissue with GT-7, GT-8, and ThioS. All GT-7 and GT-38 signal is ThioS-positive but only a subset of ThioS-positive signal is positive for GT-7 and GT-38.

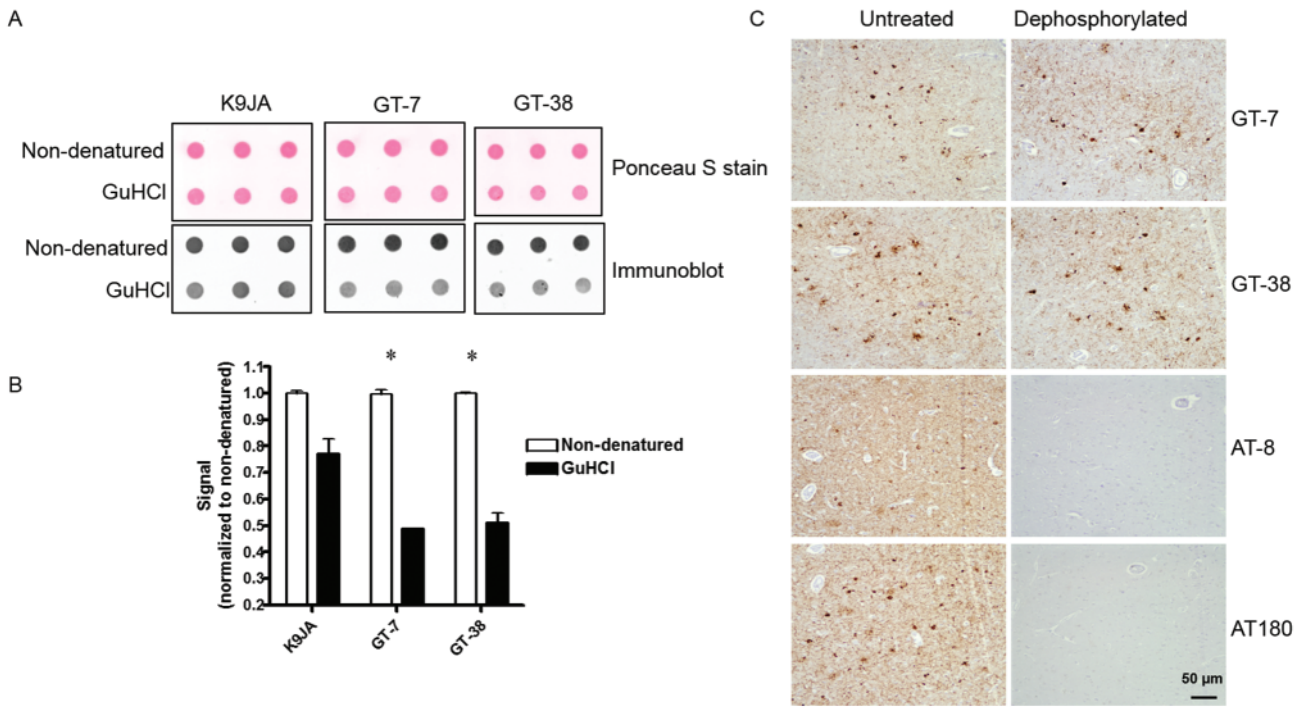

FIGURE 6. Binding of AD-selective mAbs is conformation-dependent. **(A)** Dot blot immunoreactivity of control rabbit polyclonal K9JA, and newly identified AD-selective GT-7 and GT-38 detection of brain-derived AD tau PHFs in either pathological conformation (nondenatured) or chemically denatured (GuHCl) state. **(B)** Quantification is normalized to nondenatured sample for each antibody. *$p < 0.01$ two-tailed, Student's *t*-test. **(C)** Dephosphorylation of AD tissue with λ-phosphatase and calf intestinal phosphatase demonstrates there is no change in GT-7 or GT-38 immunoreactivity by IHC.

recognize an AD-specific conformation that may correspond to an AD strain of pathological tau. Because of limited tau pathology from brains of PiD, cognitively normal, and PART patients, insufficient pathological tau extracted from these other tauopathies precluded their analyses by ELISA.

Recently, tau NFTs in the absence of Aβ plaques have been described as a distinct pathological entity, known as PART (25). However, NFTs observed in PART brains are indistinguishable from those in AD brains, which raises the question of whether the tau inclusions in PART are unique or whether they are on a pathway to AD tau pathology. Considering the relative frequency of low Braak stage tau aggregation observed in the brains of aging individuals with no clinical symptoms (who are often clinically classified as cognitively normal), we asked whether these aggregates represent a distinct benign strain of tau aggregate. Our findings here demonstrate that in both PART and patients with no cognitive impairment, tau NFTs are composed of both 3R and 4R tau isoforms and are immunoreactive for GT-7 and GT-38 suggesting that they could represent preclinical AD.

Unique tau strains have been characterized by mass spectrometric analysis of protease-resistant tau fragments isolated from human brain tissue demonstrating that CBD and PSP are 4R tauopathies while PiD is a 3R tauopathy (68–70). In practice, we observe that a portion of CBD and PSP cases have co-occurring AD tau pathology consisting of both 3R and 4R tau isoforms in areas of early deposition associated with pathological aging (e.g. locus coeruleus and transentorhinal cortex) (71). While cell type specificity, spatial distribution, and morphology allow definitive neuropathological diagnosis of tauopathies, it is not well-understood how frequently comorbid pathologies occur and how separate tauopathies may progress independently or cooperatively. We showed that GT-7 and GT-38 selectively identify AD tau pathology in the context of other co-occurring tau pathology and demonstrate that GT-7 and GT-38 are useful immunological tools for differentiating AD/aging related tau pathology from that of PiD, CBD and PSP.

Moreover, we report GT-7 and GT-38 mAbs specifically recognize ThioS-positive aggregates that contain both 3R and 4R tau isoforms. Because GT-7 was generated from a mouse immunized with AD-PFFs consisting of 90% T40 recombinant tau seeded by 10% AD-tau, we cannot rule out the possibility that the 10% AD-tau seed concomitantly induced and immunological response leading to generation of the GT-7 clone, as opposed to strictly AD-PFFs. Though 3R- and 4R-specific tau antibodies provide information about the isoform content of tau aggregates, this is the first report of an antibody that binds exclusively to AD tau pathology. Because GT-7 and GT-38 require an AD-specific fibril conformation for antibody recognition, specific epitope mapping has proved elusive. Traditional epitope mapping techniques such as peptide scanning, site-directed mutagenesis, or deletion mutants are confounded by the alternative interpretation that mutations might influence fibril conformation and may disrupt faithful recapitulation of an AD tau pathology strain. Although hydrogen-deuterium exchange mass spectrometry techniques may eventually provide insight into the precise epitope, these studies are beyond the scope of this report. However, based on the loss of immunoreactivity following chemical denaturation of tau, we can infer a complex conformation dependent epitope for GT-7 and GT-38. We further verified that binding of these mAbs is not phosphorylation-dependent based on consistent IHC staining following dephosphorylation of AD tissue. Although these findings do not rule out the possible dependence on other posttranslational modifications or cleavage events, to our knowledge there is no evidence of tauopathy specific posttranslational modifications reported for tau.

Our data here demonstrate that GT-7 and GT-38 preferentially recognize a distinct pathological AD tau conformation that is present in PART and age-matched controls with low levels of AD pathology, but do not recognize the primary diagnostic tau pathology of nonAD tauopathies in pure 3R PiD, or 4R PSP and CBD. We found that similar to AD tau, NFTs in PART and cognitively normal brain tissue contain both 3R and 4R tau isoforms and are detected by GT-7 and GT-38.

In summary, the new GT-7 and GT-38mAbs reported here will have many applications such as the identification of AD pathology in the context of co-occurring tauopathies as well as the development of AD-selective PET ligands using GT-7 and GT-38-engineered as bispecific antibodies to undergo receptor mediated transcytosis to overcome limited blood-brain barrier penetration of natural antibodies (72, 73). GT-7 and GT-38 also provide novel candidates for development of biomarker assays to identify AD-specific tau conformers in CSF of living patients with dementia. Lastly, these antibodies provide tools for assessing the faithful recapitulation of AD strain conformation in seeded fibrillization reactions of recombinant tau in vitro that will enable greater biophysical and structural characterization of tau strains.

ACKNOWLEDGMENTS

We thank John Robinson, Theresa Schuck, and Katie Casalnova for assistance with obtaining suitable brains for these studies. We thank Peter Davies for his generous gift of the MC1 and PHF1 antibodies.

REFERENCES

1. Lee VM, Goedert M, Trojanowski JQ. Neurodegenerative tauopathies. Annu Rev Neurosci 2001;24:1121–59
2. Lee VM, Brunden KR, Hutton M, et al. Developing therapeutic approaches to tau, selected kinases, and related neuronal protein targets. Cold Spring Harb Perspect Med 2011;1:a006437
3. Goedert M, Spillantini MG, Jakes R, et al. Multiple isoforms of human microtubule-associated protein tau: Sequences and localization in neurofibrillary tangles of Alzheimer's disease. Neuron 1989;3:519–26
4. Ballatore C, Lee VM, Trojanowski JQ. Tau-mediated neurodegeneration in Alzheimer's disease and related disorders. Nat Rev Neurosci 2007;8:663–72
5. Yoshiyama Y, Lee VM, Trojanowski JQ. Therapeutic strategies for tau mediated neurodegeneration. J Neurol Neurosurg Psychiatry 2013;84:784–95
6. Mandelkow E, von Bergen M, Biernat J, et al. Structural principles of tau and the paired helical filaments of Alzheimer's disease. Brain Pathol 2007;17:83–90
7. Guerrero-Munoz MJ, Gerson J, Castillo-Carranza DL. Tau oligomers: The toxic player at synapses in Alzheimer's disease. Front Cell Neurosci 2015;9:464
8. Goedert M, Jakes R. Mutations causing neurodegenerative tauopathies. Biochim Biophys Acta 2005;1739:240–50
9. Dickson DW, Kouri N, Murray ME, et al. Neuropathology of frontotemporal lobar degeneration-tau (FTLD-tau). J Mol Neurosci 2011;45:384–9

10. Spillantini MG, Goedert M. Tau pathology and neurodegeneration. Lancet Neurol 2013;12:609–22
11. Irwin DJ, Cairns NJ, Grossman M, et al. Frontotemporal lobar degeneration: Defining phenotypic diversity through personalized medicine. Acta Neuropathol 2015;129:469–91
12. Braak H, Braak E. Neuropathological stageing of Alzheimer-related changes. Acta Neuropathol 1991;82:239–59
13. Buee L, Delacourte A. Comparative biochemistry of tau in progressive supranuclear palsy, corticobasal degeneration, FTDP-17 and Pick's disease. Brain Pathol 1999;9:681–93
14. Arima K. Ultrastructural characteristics of tau filaments in tauopathies: Immuno-electron microscopic demonstration of tau filaments in tauopathies. Neuropathology 2006;26:475–83
15. Ksiezak-Reding H, Morgan K, Mattiace LA, et al. Ultrastructure and biochemical composition of paired helical filaments in corticobasal degeneration. Am J Pathol 1994;145:1496–508
16. Mott RT, Dickson DW, Trojanowski JQ, et al. Neuropathologic, biochemical, and molecular characterization of the frontotemporal dementias. J Neuropathol Exp Neurol 2005;64:420–8
17. Boluda S, Iba M, Zhang B, et al. Differential induction and spread of tau pathology in young PS19 tau transgenic mice following intracerebral injections of pathological tau from Alzheimer's disease or corticobasal degeneration brains. Acta Neuropathol 2015;129:221–37
18. Clavaguera F, Akatsu H, Fraser G, et al. Brain homogenates from human tauopathies induce tau inclusions in mouse brain. Proc Natl Acad Sci USA 2013;110:9535–40
19. Brettschneider J, Del Tredici K, Lee VM, et al. Spreading of pathology in neurodegenerative diseases: A focus on human studies. Nat Rev Neurosci 2015;16:109–20
20. Guo JL, Lee VM. Cell-to-cell transmission of pathogenic proteins in neurodegenerative diseases. Nat Med 2014;20:130–8
21. Goedert M, Spillantini MG. Propagation of Tau aggregates. Mol Brain 2017;10:18
22. Reilly P, Winston CN, Baron KR, et al. Novel human neuronal tau model exhibiting neurofibrillary tangles and transcellular propagation. Neurobiol Dis 2017;106:222–34
23. Narasimhan S, Guo JL, Changolkar L, et al. Pathological tau strains from human brains recapitulate the diversity of tauopathies in nontransgenic mouse brain. J Neurosci 2017;37:11406–23
24. Fitzpatrick AWP, Falcon B, He S, et al. Cryo-EM structures of tau filaments from Alzheimer's disease. Nature 2017;547:185–90
25. Crary JF, Trojanowski JQ, Schneider JA, et al. Primary age-related tauopathy (PART): A common pathology associated with human aging. Acta Neuropathol 2014;128:755–66
26. Itoh Yamada M, Yoshida R, et al. Dementia characterized by abundant neurofibrillary tangles and scarce senile plaques: A quantitative pathological study. Eur Neurol 1996;36:94–7
27. Santa-Maria I, Haggiagi A, Liu X, et al. The MAPT H1 haplotype is associated with tangle-predominant dementia. Acta Neuropathol 2012;124:693–704
28. Duyckaerts C, Braak H, Brion JP, et al. PART is part of Alzheimer disease. Acta Neuropathol 2015;129:749–56
29. Guo JL, Narasimhan S, Changolkar L, et al. Unique pathological tau conformers from Alzheimer's brains transmit tau pathology in nontransgenic mice. J Exp Med 2016;213:2635–54
30. Jicha GA, Bowser R, Kazam IG, et al. Alz-50 and MC-1, a new monoclonal antibody raised to paired helical filaments, recognize conformational epitopes on recombinant tau. J Neurosci Res 1997;48:128–32
31. Carmel G, Mager EM, Binder LI, et al. The structural basis of monoclonal antibody Alz50's selectivity for Alzheimer's disease pathology. J Biol Chem 1996;271:32789–95
32. Ghoshal N, Garcia-Sierra F, Fu Y, et al. Tau-66: Evidence for a novel tau conformation in Alzheimer's disease. J Neurochem 2001;77:1372–85
33. Jicha GA, Lane E, Vincent I, et al. A conformation- and phosphorylation-dependent antibody recognizing the paired helical filaments of Alzheimer's disease. J Neurochem 1997;69:2087–95
34. Vincent I, Jicha G, Rosado M, et al. Aberrant expression of mitotic cdc2/cyclin B1 kinase in degenerating neurons of Alzheimer's disease brain. J Neurosci 1997;17:3588–98
35. Yoshida M. Cellular tau pathology and immunohistochemical study of tau isoforms in sporadic tauopathies. Neuropathology 2006;26:457–70
36. Bell K, Cairns NJ, Lantos PL, et al. Immunohistochemistry distinguishes: Between Pick's disease and corticobasal degeneration. J Neurol Neurosurg Psychiatry 2000;69:835–6
37. Zhukareva V, Mann D, Pickering-Brown S, et al. Sporadic Pick's disease: A tauopathy characterized by a spectrum of pathological tau isoforms in gray and white matter. Ann Neurol 2002;51:730–9
38. Irwin DJ, Brettschneider J, McMillan CT, et al. Deep clinical and neuropathological phenotyping of Pick disease. Ann Neurol 2016;79:272–87
39. Lee VM, Balin BJ, Otvos L, Jr., et al. A68: A major subunit of paired helical filaments and derivatized forms of normal Tau. Science 1991;251:675–8
40. Lee VMY, Wang J, Trojanowski JQ. Purification of paired helical filament tau and normal tau from human brain tissue. Method Enzymol 1999;309:81–9
41. Guo JL, Lee VM. Seeding of normal Tau by pathological Tau conformers drives pathogenesis of Alzheimer-like tangles. J Biol Chem 2011;286:15317–31
42. Li W, Lee VM. Characterization of two VQIXXK motifs for tau fibrillization in vitro. Biochemistry 2006;45:15692–701
43. Covell DJ, Robinson JL, Akhtar RS, et al. Novel conformation-selective alpha-synuclein antibodies raised against different in vitro fibril forms show distinct patterns of Lewy pathology in Parkinson's disease. Neuropathol Appl Neurobiol 2017;43:604–20
44. Arnold SE, Toledo JB, Appleby DH, et al. Comparative survey of the topographical distribution of signature molecular lesions in major neurodegenerative diseases. J Comp Neurol 2013;521:4339–55
45. Toledo JB, Van Deerlin VM, Lee EB, et al. A platform for discovery: The University of Pennsylvania Integrated Neurodegenerative Disease Biobank. Alzheimers Dement 2014;10:477–84.e1
46. Kovacs GG, Robinson JL, Xie SX, et al. Evaluating the patterns of aging-related tau astrogliopathy unravels novel insights into brain aging and neurodegenerative diseases. J Neuropathol Exp Neurol 2017;76:270–88
47. Irwin DJ, Cohen TJ, Grossman M, et al. Acetylated tau neuropathology in sporadic and hereditary tauopathies. Am J Pathol 2013;183:344–51
48. Schmidt ML, Schuck T, Sheridan S, et al. The fluorescent Congo red derivative, (trans, trans)-1-bromo-2, 5-bis-(3-hydroxycarbonyl-4-hydroxy)styrylbenzene (BSB), labels diverse beta-pleated sheet structures in postmortem human neurodegenerative disease brains. Am J Pathol 2001;159:937–43
49. Irwin DJ, Lleo A, Xie SX, et al. Ante mortem CSF tau levels correlate with post mortem tau pathology in FTLD. Ann Neurol 2017;82:247–252.
50. Mondragon-Rodriguez S, Basurto-Islas G, Santa-Maria I, et al. Cleavage and conformational changes of tau protein follow phosphorylation during Alzheimer's disease. Int J Exp Pathol 2008;89:81–90
51. Xu S, Brunden KR, Trojanowski JQ, et al. Characterization of tau fibrillization in vitro. Alzheimers Dement 2010;6:110–7
52. Lee VMY, Balin BJ, Otvos L, et al. A68 – A major subunit of paired helical filaments and derivatized forms of normal-tau. Science 1991;251:675–8
53. Alonso AC, Grundke-Iqbal I, Iqbal K. Alzheimer's disease hyperphosphorylated tau sequesters normal tau into tangles of filaments and disassembles microtubules. Nat Med 1996;2:783–7
54. Wagner U, Utton M, Gallo JM, et al. Cellular phosphorylation of tau by GSK-3 beta influences tau binding to microtubules and microtubule organisation. J Cell Sci 1996;109:1537–43
55. Yoshiyama Y, Higuchi M, Zhang B, et al. Synapse loss and microglial activation precede tangles in a P301S tauopathy mouse model. Neuron 2007;53:337–51
56. Lee G, Thangavel R, Sharma VM, et al. Phosphorylation of tau by fyn: Implications for Alzheimer's disease. J Neurosci 2004;24:2304–12
57. Otvos L, Jr., Feiner L, Lang E, et al. Monoclonal antibody PHF-1 recognizes tau protein phosphorylated at serine residues 396 and 404. J Neurosci Res 1994;39:669–73
58. Vandermeeren M, Lubke U, Six J, et al. The phosphatase inhibitor okadaic acid induces a phosphorylated paired helical filament tau epitope in human LA-N-5 neuroblastoma cells. Neurosci Lett 1993;153:57–60
59. Mercken M, Vandermeeren M, Lubke U, et al. Monoclonal antibodies with selective specificity for Alzheimer Tau are directed against phosphatase-sensitive epitopes. Acta Neuropathol 1992;84:265–72
60. Binder LI, Guillozet-Bongaarts AL, Garcia-Sierra F, et al. Tau, tangles, and Alzheimer's disease. Biochim Biophys Acta 2005;1739:216–23

61. Guillozet-Bongaarts AL, Glajch KE, Libson EG, et al. Phosphorylation and cleavage of tau in non-AD tauopathies. Acta Neuropathol 2007;113: 513–20
62. Berry RW, Sweet AP, Clark FA, et al. Tau epitope display in progressive supranuclear palsy and corticobasal degeneration. J Neurocytol 2004;33: 287–95
63. Irwin DJ, Cohen TJ, Grossman M, et al. Acetylated tau, a novel pathological signature in Alzheimer's disease and other tauopathies. Brain 2012; 135:807–18
64. Novak M, Wischik CM, Edwards P, et al. Characterisation of the first monoclonal antibody against the pronase resistant core of the Alzheimer PHF. Prog Clin Biol Res 1989;317:755–61
65. Guillozet-Bongaarts AL, Garcia-Sierra F, Reynolds MR, et al. Tau truncation during neurofibrillary tangle evolution in Alzheimer's disease. Neurobiol Aging 2005;26:1015–22
66. Min SW, Cho SH, Zhou Y, et al. Acetylation of tau inhibits its degradation and contributes to tauopathy. Neuron 2010;67:953–66
67. Cohen TJ, Guo JL, Hurtado DE, et al. The acetylation of tau inhibits its function and promotes pathological tau aggregation. Nat Commun 2011; 2:252
68. Taniguchi-Watanabe S, Arai T, Kametani F, et al. Biochemical classification of tauopathies by immunoblot, protein sequence and mass spectrometric analyses of sarkosyl-insoluble and trypsin-resistant tau. Acta Neuropathol 2016;131:267–80
69. Delacourte A, Sergeant N, Wattez A, et al. Vulnerable neuronal subsets in Alzheimer's and Pick's disease are distinguished by their tau isoform distribution and phosphorylation. Ann Neurol 1998;43:193–204
70. Sergeant N, Wattez A, Delacourte A. Neurofibrillary degeneration in progressive supranuclear palsy and corticobasal degeneration: Tau pathologies with exclusively "exon 10" isoforms. J Neurochem 1999;72:1243–9
71. Braak H, Del Tredici K. The pathological process underlying Alzheimer's disease in individuals under thirty. Acta Neuropathol 2011;121: 171–81
72. Sehlin D, Fang XT, Cato L, et al. Antibody-based PET imaging of amyloid beta in mouse models of Alzheimer's disease. Nat Commun 2016;7: 10759
73. Webster CI, Caram-Salas N, Haqqani AS, et al. Brain penetration, target engagement, and disposition of the blood-brain barrier-crossing bispecific antibody antagonist of metabotropic glutamate receptor type 1. FASEB J 2016;30:1927–40